Effects of concrete composition on the interfacial parameters governing FRP debonding from the concrete substrate

J.L. Pan
Key Laboratory of Concrete and Prestressed Concrete Structure, Ministry of Education
Southeast University, China
C. K.Y. Leung
Hong Kong University of Science and Technology, Hong Kong

ABSTRACT: For the concrete beam strengthened with FRP, failure may occur from the bottom of a major flexural/shear crack along the span. As debonding failure occurs within the concrete, interfacial friction resulted from aggregate interlocking between opposing surfaces of the debonded zone plays an important role in the debonding behavior. Interfacial debonding can be analyzed with a three-parameter model. To investigate the effect of concrete composition on debonding behavior, the direct shear test was conducted with ten different compositions of concrete. Interfacial parameters were then derived according to a three-parameter model. The test results show little correlation between interfacial parameters and concrete compressive or splitting tensile strength. However, the debonding initiation strength and residual shear strength correlates well with the surface tensile strength and the maximum crack opening is mainly governed by the aggregate content. According to our results, the composition of the concrete is an important factor that should be considered explicitly in the investigation of FRP debonding from a concrete substrate.

1 INTRODUCTION

The continuous aging of civil infrastructures and the change of load requirements with time give rise to the need of structural strengthening. The bonding of fiber reinforced plastics (FRP) plates on concrete members has been recognized as an effective retrofitting technique. For concrete beams strengthened with FRP, debonding failure may occur from the bottom of a major flexural/shear crack in the span, as shown in Fig.1. This kind of crack-induced debonding is initiated by the presence of high shear stress concentration at the interface around the bottom of the cracks. As debonding failure occurs within the concrete substrate at a small distance from the concrete/adhesive interface, interfacial friction resulted from aggregate interlocking between opposing surfaces of the debonded zone plays an important role in the debonding behavior.

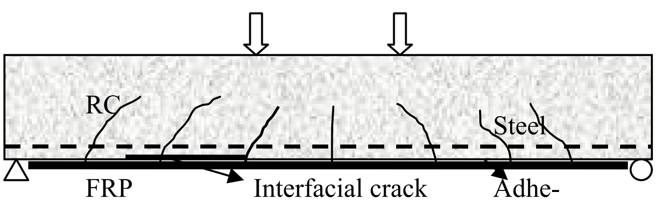

Fig.1 FRP debonding from the bottom of a major flexural/shear crack

Crack-induced debonding failure is often studied with the direct shear test, which involves a FRP plate bonded on a concrete prism. By pulling the FRP plate along the direction of its length, the bond capacity at debonding failure can be obtained. Due to the shear lag phenomenon, the bond capacity approaches a plateau value with increasing bond length. Recently, plenty of experiments have been conducted with single shear tests (e.g. Taljsten 1997, Chajes et al. 1996, Bizindavyi and Neale 1999), double shear tests (e.g. Van Gemert 1980, Neubauer and Rostásy 1997) and modified beam (e.g. Van Gemert 1980, de Lorenzis et al. 2001) to study the bond behavior between FRP and concrete members. These works have led to improved understanding of the failure characteristics of the FRP-to-concrete bond. It is commonly considered that the effectiveness of strengthening depends on the following aspects: (1) surface preparation of concrete; (2) the type of adhesive; (3) geometric factors, such as FRP bond length, thickness of FRP plate, FRP width etc; (4) interfacial fracture energy. The interfacial fracture energy is often taken to be a function of the compressive or tensile strength of concrete. However, a systematic study on the correlation between the fracture energy and these strength parameters has never been performed. Also, to analyze the debonding process, various investigators have developed models (Holzenkampfer 1994, Yuan et al. 2001, Chen and Teng 2001) based on nonlinear fracture mechanics concepts. The debonded zone is treated as a process zone with residual shear stress, which decreases with interfacial sliding due to effect of abrasion. As aggregate interlocking is related to the size and content of the aggregates in the concrete, the debonding behavior is expected to be affected by the concrete composition, in addition to macroscopic mechanical properties such as compressive and splitting tensile strength.

In the present investigation, the direct shear test is performed on concrete prisms with bonded FRP to study the interfacial debonding behavior. Various strength parameters of the concrete as well as its aggregate content are also measured. The objective of this study is to investigate the effect of (1) concrete properties (such as concrete compressive strength, splitting tensile strength, and concrete surface strength), and (2) the aggregate content, on the debonding behavior. In the testing program, concrete of 10 different compositions are employed. Interfacial debonding is analyzed with a three-parameter model, in which debonding is assumed to initiate once the interfacial shear stress reaches a critical value τ_s. After the initiation of debonding, the interfacial stress drops to a lower value τ_0. On further sliding, the stress will decrease with interfacial sliding at a slope k. Using such a model, the variation of stress and strain along the FRP during the debonding process can be derived. By fitting the theoretical FRP strain distribution to measured values on various specimens, the three model parameters (τ_s, τ_0, k) can be obtained for each concrete composition. The correlations between interfacial parameters and strength parameters as well as aggregate content are then studies, and empirical relations are proposed.

2 EXPERIMENTAL PROGRAM

2.1 *Specimen Preparation and Material Properties*

To investigate the effect of concrete composition on the debonding behavior, ten batches of concrete with different mixing proportions were employed to prepare the concrete prisms. The mixing proportions for each batch of specimens are listed in Table 1. The size of the concrete prism is 100mm (width) x100mm (depth) x500mm (length), as shown in Figure 2. After casting, the specimens were placed in the curing room for 28 days. After curing, FRP sheets can be applied. Before FRP bonding, the surfaces of concrete prisms were roughened with a needle-gun to expose the aggregates so that a good bond between FRP plate and concrete could be achieved. After the surface preparation, epoxy primer, which is a cohesive liquid at atmosphere temperature, was applied to improve the bond performance. After the primer was hardened, two layers of FRP sheets were bonded to concrete prisms layer by layer using epoxy resin. The bonded part of the FRP plate was 300mm in extent, starting from a location 50mm from the edge of concrete prism (Fig.2). The initial 50mm is left unbonded to avoid wedge failure of concrete due to shear stress. To ensure full hardening of epoxy, the specimens should be cured for 7 days before testing. In order to record the strain variation along the FRP plate during the loading process, nine strain gauges were placed on the FRP plate with a center-to-center space of 30mm, as shown in Fig.2. For the acquisition of strain data, an automatic data logger was employed.

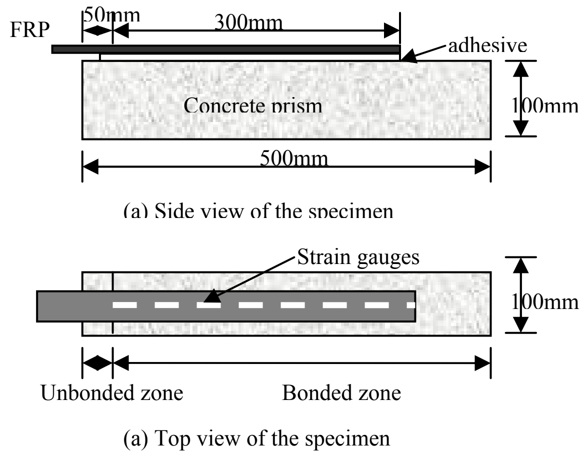

Fig.2 Dimensional information about the specimens

To study the correlations between the concrete material properties and the debonding behavior, the mechanical properties of concrete, including compressive strength, tensile strength and surface tensile strength, were measured together with the ultimate bond capacity. Three small concrete cylinders (100mm in diameter and 200mm in height) from each batch of concrete were used to obtain the compressive strength, and another three concrete cylinders with larger size (150mm in diameter and 300mm in height) were used to perform splitting tension test. To measure surface tensile strength, a steel plate with dimension of 100mmx100mm was bonded on the concrete prism. The surface tensile strength is then calculated as the ultimate load divided by the total area of the steel plate. In addition, the aggregate content was measured as the area fraction of aggregates (defined as particles with projected dimension larger than 4.75mm) on the concrete section. The various material properties of the concrete are summarized in Table 1. The FRP used in the tests is the Reno composite material system, with strength of 4200MPa in the fiber direction. The Young's modulus of the FRP is about 235GPa. The FRP thickness is about 0.11mm per ply according to the production specifications and two plies were employed in the test specimen. In the present experiments, an epoxy-based adhesive was used. According to the manufacturer, the tensile strength of the resin for FRP is about 30MPa, the tensile modulus is about 3.3GPa and shear strength is over 10MPa after curing for 7 days.

Table 1 Experimental results of material properties of the concrete

concrete composition	Mixing Proportion (C:W:S:A)	Aggregate content	Compr. Strength (MPa)	Tensile Strength (MPa)	Surface tensile strength (MPa)
M1	1:0.5:1.5:2.6	0.119	43.1	4.18	2.851
M2	1:0.6:1.5:2.6	0.107	35.2	3.17	2.146
M3	1:0.5:1.5:1.5	0.117	57.5	3.69	3.04
M4	1:0.6:1.5:1.5	0.091	38.6	3.38	1.625
M5	1:0.4:1.5:2.6	0.096	61.5	4.48	2.779
M6	1:0.5:1.5:0.5	0.036	47.4	3.76	2.261
M7	1:0.54:2.55:1	0.030	47.13	3.68	2.037
M8	1:0.5:2.25:1.25	0.070	44.73	3.26	2.225
M9	1:0.5:2:1.5	0.103	52.35	3.99	2.730
M10	1:0.5:1.5:2	0.118	57.87	4.49	2.474
Remarks	C:W:S:A is the ratio of cement to water to sand to aggregate				

2.2 *Test Setup and Test Procedure*

As for the setup of the direct shear test, a steel frame that can hold the concrete specimen tightly in the vertical direction was designed. The frame was vertically installed in the MTS loading frame that applied a pulling force on the FRP plate. Alignment is important as the force should be along the vertical direction to prevent any horizontal force component that may introduce peeling effect on the FRP plate. During the testing process, a LVDT is used to measure the global displacement of the FRP plate. The test was conducted under displacement control with loading rate of 0.1mm/min. An automatic data logger was employed to collect the strains along the FRP plate and the displacement from the LVDT, as well as load and stroke data from the MTS machine.

2.3 *Strain distributions during the loading process*

In the experimental program, a total of 30 specimens (10 for each concrete composition) were tested to investigate the effect of concrete composition on the bond behavior between the FRP plate and concrete. For each group of specimens with the same concrete composition, one specimen was instrumented with nine strain gauges for measuring strain variations during the loading process. Only two strain gauges were put on the other two specimens for checking.

To illustrate the debonding behavior for the specimens under direct shear force, the experimental data of the specimen M7-2 is shown as an example. Fig.3 shows the strain distributions along the FRP plate at different load values. Each curve corresponds to the strain distribution along the FRP at a particular load. When the load is lower than 8kN, the strains in the FRP plate decrease quickly with distance from the loaded end. This descending trend is ascribed to the low axial stiffness of the bonded FRP plate with respect to that of the concrete prism. Before initial debonding, increase of the applied load will cause the curve to shift upward, but the shape of the strain distribution doesn't change. However, when the load value goes beyond 8kN, the interfacial debonding starts to occur from the loaded end, and the shape of the curve starts to change and the slope of the curve near the loaded end tends to decrease. Since the slope of the curve reflects the rate of strain change in the FRP plate (which is proportional to the interfacial shear stress), the decrease of the slope represents shear softening along the debonded interface. As the load increases, the interfacial debonding tends to propagate to the free end of the FRP plate. This is indicated by the shifting of strain distribution curves towards the free end of the FRP plate. Interestingly, it is found that the maximum strain in the FRP plate stays approximately constant when the debonded zone has extended to a certain distance from the pulled end. This corresponds to the situation with a fully developed debonding zone propagating along the interface.

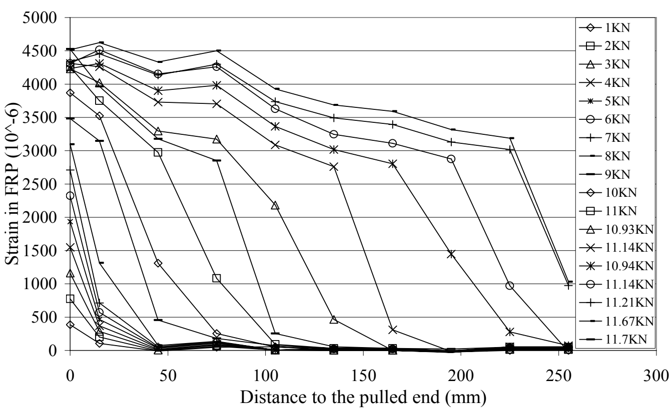

Fig.3 Strain variations at different load values for the specimen M8-2

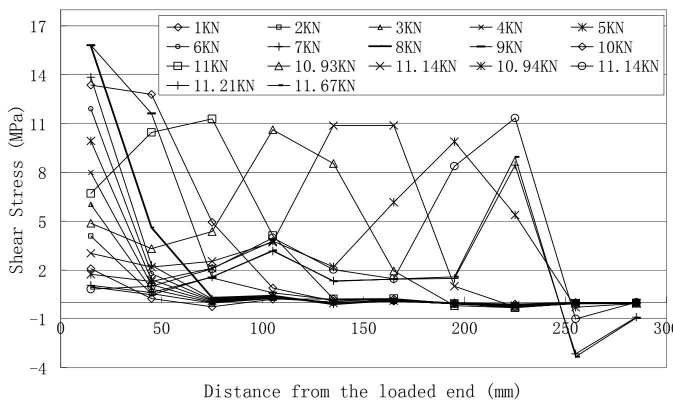

Fig.4 Shear stress distributions along the concrete/adhesive interface for M7-2

Fig.4 shows the approximate shear stress distributions along the concrete/adhesive interface at different load values. The shear stress at each location is calculated as the difference between the tensile stresses at adjacent points divided by the distance between the two points. With this approximate calculation method, the magnitude of the shear stress is not accurate, but the trend of shear stress variation with increased loading can still be revealed. When the applied load is smaller than 8kN, the shear stress is found to decrease quickly with the distance from the loaded end. When the loading goes beyond 8kN, location of τ_{max} shifts towards the free end of the plate, indicating the debonding process of the FRP plate from the concrete substrate. As loading continues to increase, the shear stress at points near the pulled end show a decreasing trend, indicating shear softening along the interface in the debonded region.

3 THEORETICAL MODELINNG

3.1 Interfacial shear softening relation

To model interfacial debonding, the shear slip relation along the concrete/adhesive interface is required. With a proper bond shear slip relation, the theoretical stresses or strains along the FRP plate and the interfacial stresses along the concrete/adhesive interface can be obtained. In the present study, the three-parameter model proposed by Leung and Tung (2006) is employed to study debonding behavior. In the model, interfacial debonding is taken to start when the interfacial shear stress at the concrete/adhesive interface reaches the interfacial shear strength τ_s. After debonding, the residual shear strength (τ_0) at the concrete/adhesive interface is related to the interfacial sliding by:

$$\tau = \tau_0 - ks \tag{1}$$

where τ_0 and k are initial residual shear strength right after debonding and softening rate in the debonded zone. Based on this interfacial softening relation, the tensile stress or strain distribution along the FRP plate and interfacial shear stress distribution along the concrete/adhesive interface can be derived. Details of the derivation can be found in Leung and Tung (2006).

3.2 *Interfacial Parameters for Various Concrete Compositions*

To illustrate the extraction of interfacial parameters, results for specimen M7-2 is employed. With the three-paramter model, the tensile strain along the FRP plate at different load values are calculated and compared with the test results (Fig.5). The actual interfacial parameters are the ones that provide good agreement between calculated and measured strain.

Due to the irregular surface of the concrete after roughening, it is very difficult to measure the adhesive thickness accurately. The mean thickness of adhesive layer is therefore obtained by the fitting of strain distributions along the FRP plate within the elastic stage. Good agreement between calculated and experimental results is obtained when the adhesive thickness is taken to be about 3mm, as shown in Fig.5a. The maximum shear stress (τ_s) is determined from the highest applied loading before the elastic stress distribution starts to shift towards the free end of the plate. By fitting the tensile strains along the FRP plate in the nonlinear regime (Fig.5b), the residual shear strength (τ_0) and the softening rate (k) can be obtained. The maximum sliding is calculated as $\delta=\tau_0/k$, which signifies the sliding distance beyond which the residual stress drops to zero.

The fitting process has been repeated for all specimens of different concrete compositions. The derived adhesive thickness and interfacial parameters are shown in Table 2. For each specimen, the adhesive thickness is found to be in the range from 3mm to 3.5mm, which is consistent with visual inspection.

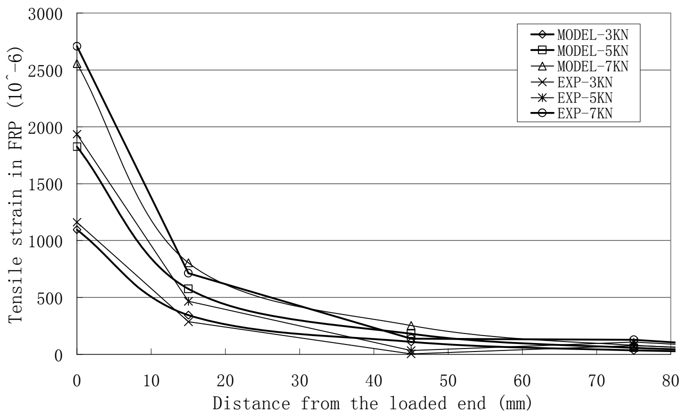

(a)

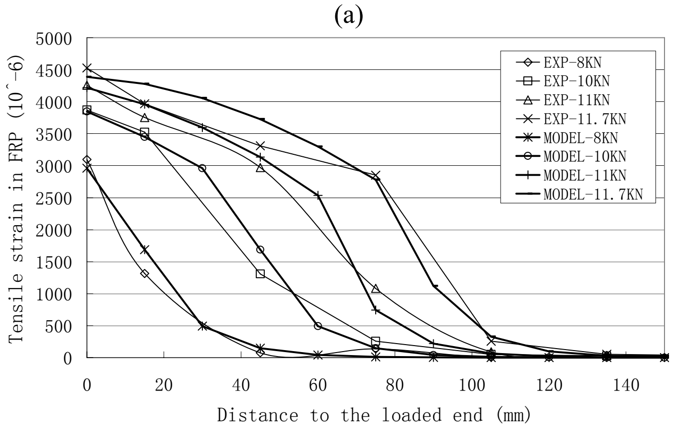

(b)

Fig. 5 Comparisons between the fitting results and test results (a) before initial debonding (b) after initial debonding

3.3 Correlations between concrete properties and interfacial shear strength

To study the effect of concrete properties on the debonding behavior, the interfacial shear strength is correlated to the macroscopic properties of concrete. According to the test results, the compressive strength of concrete for each batch ranges from 35.2MPa to 61.5MPa. The splitting tensile strength values of the concrete are between 3.17MPa and 4.49MPa. The surface tensile strength for each concrete composition varies from 1.625MPa to 3.04MPa. Fig.6 shows the correlations between the interfacial shear strength and concrete material properties. According to the plots, the interfacial shear strength has the best correlation with surface tensile strength of concrete. There is also some correlation with the compressive strength, but not as good as that with the surface tensile strength. No clear correlation can be found between the interfacial shear strength and the splitting tensile strength, as well as the aggregate content. According to the test results, it seems that debonding initiation, which is induced by forces acting on the concrete surface only, is not affected by the bulk material properties of the specimen. Also, the aggregate content, which does not govern the surface strength of concrete, has little correlation with the interfacial shear strength.

Table 2 Simulation results of the adhesive thickness and interfacial parameters

	Adhesive Thickness (mm)	τ_{max} (MPa)	τ_0 (MPa)	k (MPa/mm)	Max. crack opening(mm)	Exp.P_{ult} (kN)
M1-2	3	16.0	2.5	2.3	1.09	17.46
M2-3	3	13.5	1.6	2.0	0.8	14.75
M3-2	3	17.8	1.8	2.0	0.9	19.43
M4-3	3.5	13.0	1.5	2.3	0.65	15.68
M5	--	--	--	--	--	17.45
M6-3	3.5	14.7	1.5	2.5	0.6	13.31
M7-2	3	11.3	2.0	6.0	0.33	11.71
M8-3	3	13.8	1.3	2.0	0.65	13.07
M9-2	3	16.2	2.0	3.5	0.57	17.48
M10-2	3	15.8	1.8	2.5	0.72	18.07

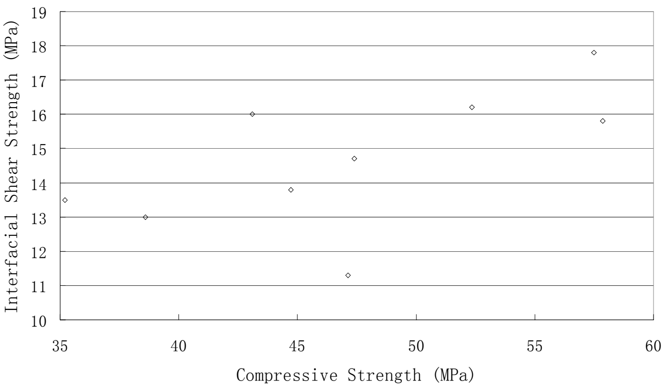

(a)

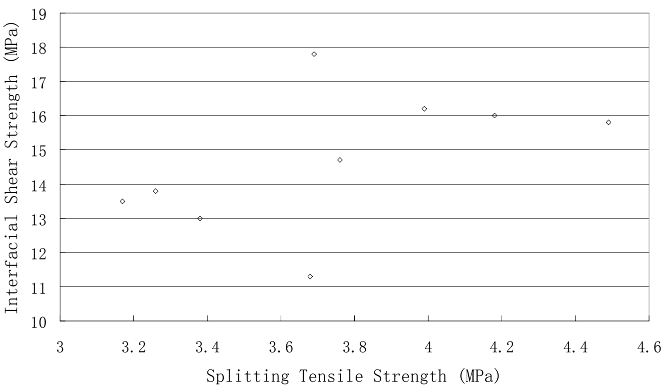

(b)

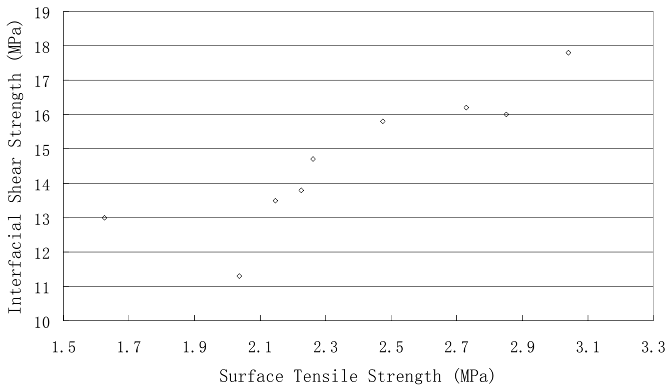

(c)

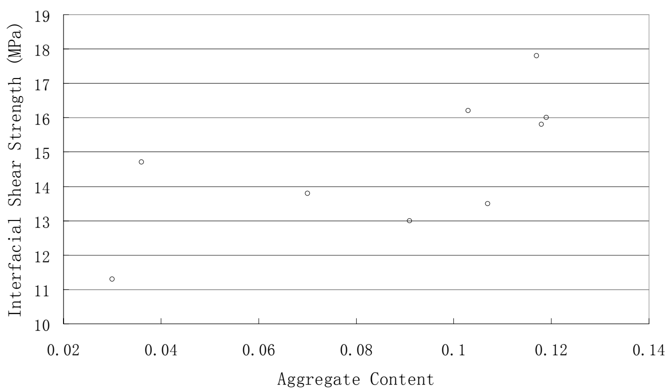

(d)

Fig.6 Correlation between the interfacial shear strength and (a) compressive strength, (b) splitting tensile strength, (c) surface tensile strength, (d) aggregate content

Based on the above, an empirical equation for the interfacial shear strength can be proposed as:

$$\tau_s = 3.92 f_{ctm} + 5.36 \qquad (2)$$

where 'f_{ctm}' is the concrete surface tensile strength from pull-out test.

3.4 Correlations between residual debonding strength and the concrete properties

As mentioned above, the FRP debonding failure in the direct shear test can be analyzed with the three-parameter model, and the interfacial parameters are obtained by the data fitting with experimental results. The residual shear strength defines the interfacial shear friction between the FRP plate and the concrete right after debonding. It is one of the key parameters determining the debonding behavior. To study the effect of concrete properties on the debonding behavior, the correlations between the residual shear strength and the concrete properties are plotted in Fig.7. It is found that the residual shear strength has good correlation with the splitting tensile strength and surface tensile strength of concrete, but has little correlation with concrete compressive strength or aggregate content.

To quantify the effect of concrete properties on the debonding behavior, the residual shear strength is related to the surface tensile strength of concrete f_{ctm} only, and the residual shear strength τ_0 can be given by:

$$\tau_0 = 0.457 f_{ctm} + 0.692 \qquad (3)$$

where f_{ctm} is the concrete surface tensile strength from pull-out test.

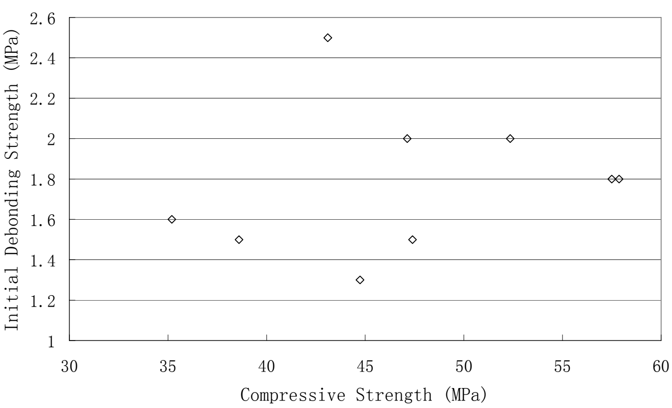

(a)

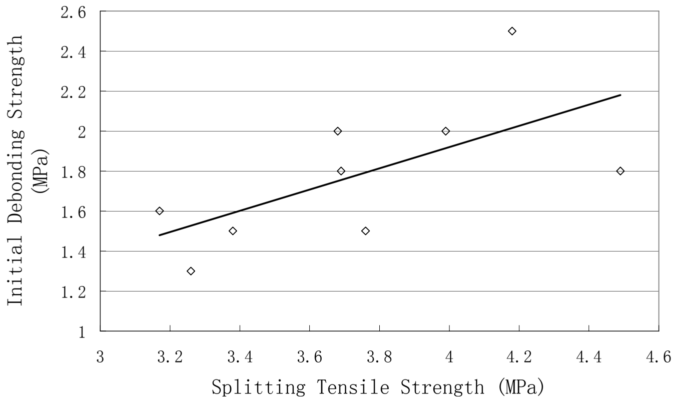

(b)

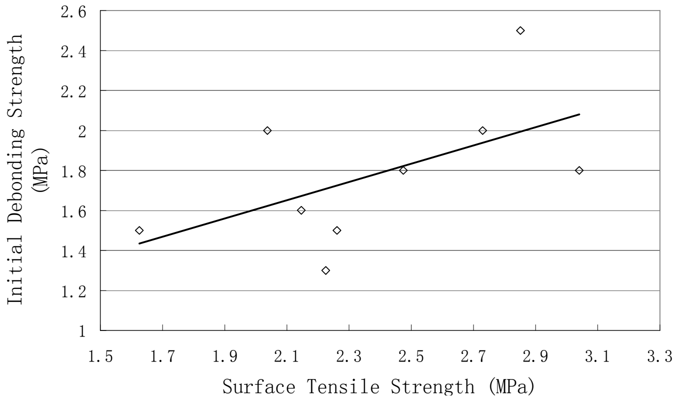

(c)

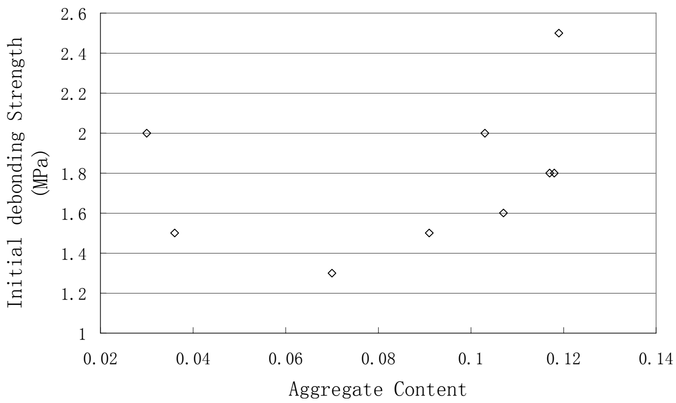

(d)

Fig.7 Correlation between the residual debonding strength and (a) compressive strength, (b) splitting tensile strength, (c) surface tensile strength, (d) aggregate content

3.5 Correlations between the maximum crack opening and the concrete properties

The maximum sliding ($\delta=\tau_0/k$) defines the maximum relative displacement within which interfacial friction still exists between the FRP plate and the concrete. The maximum sliding is an important parameter for analyzing the shear softening in the debonded zone. In Fig.8, the maximum sliding is plotted against the concrete properties. The results indicate that this parameter correlates better with the surface tensile strength and aggregate content than the compressive or splitting tensile strength of concrete. The strong effect of aggregate content on the maximum crack opening may be resulting from the fact that a higher aggregate content increases the abrasion resistance along the interface and hence delay the shear softening between the FRP and the concrete. The surface tensile strength reflects the quality of concrete surface, and hence it will affect the abrasion behavior during the debonding process. To quantify the effect of aggregate content and surface tensile strength, the maximum sliding is modeled with these two parameters. According to linear regression analysis, the empirical model of the maximum crack opening ‘δ’ in terms of the surface tensile strength ‘f_{ctm}’ and aggregate content ‘a’ is given by:

$$\delta = f_{ctm}^{2.6}(-0.583a+0.135) \tag{4}$$

Note that δ is an important parameter governing the maximum bond force that can be sustained by the FRP. With a high value of δ, a large softening zone can be formed along the interface, resulting in a high load at ultimate debonding failure.

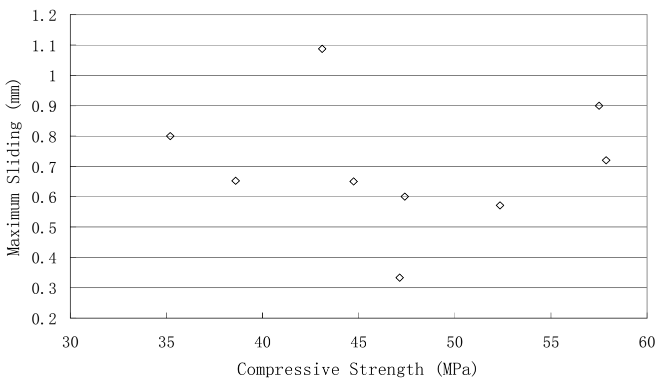

(a)

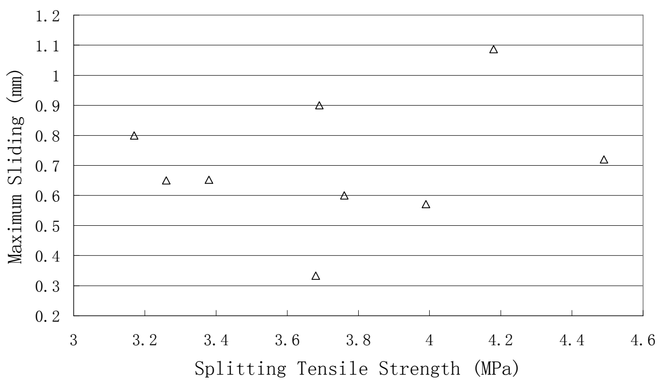

(b)

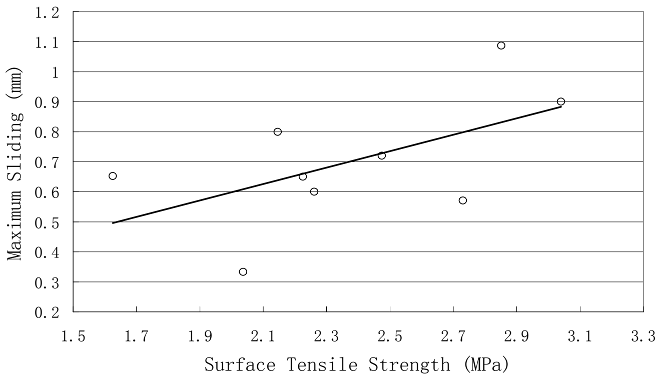

(c)

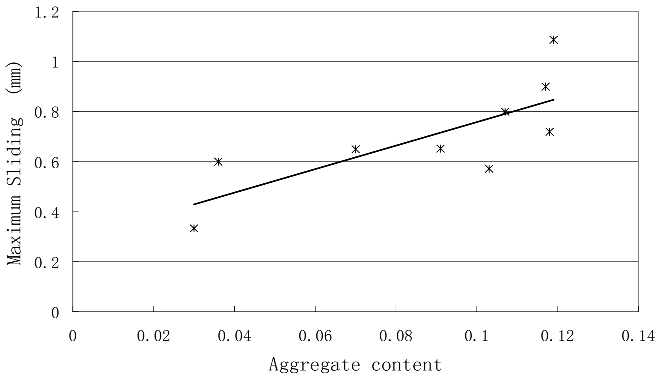

(d)

Fig.8 Correlation between the maximum sliding crack opening and (a) compressive strength, (b) splitting tensile strength, (c) surface tensile strength, (d) aggregate content

3.6 Determination of ultimate bond capacity with the empirical equations

Using Eqns (2) to (4) derived above, the interfacial parameters for each composition is empirically related to the surface tensile strength and aggregate content. With these parameters, the ultimate bond capacity is derived using the 3-parameter debonding model (with $k=\tau_0/\delta$). The calculated load capacities are compared with the experimental results in Fig.9. Most data points locate near the 45-degree line and within the error range of positive and negative 10 percentages. Only one data point locates at the error line of 20 percentages, which may be resulted from the inconsistency of test data. Generally speaking, the bond capacity is reasonably predicted with parameters derived from the proposed empirical equations.

Since the same data in Fig.9 has been used to derive the empirical equations, the comparison in Fig.9 is not an independent validation of the equations. We want to point out, however, that if the aggregate content has not been included in Eqn (4), the resulting fitting will show a much larger coefficient of variation. As a result, the calculated bond capacity will also not be in good agreement with the test results. Our investigation therefore establishes the aggregate content to be an important parameter governing debonding behavior. In other words, the effect of concrete composition should not be neglected in the study of debonding along the FRP/concrete interface.

3.7 Further Discussions

The current investigation is certainly far from complete. The proposed empirical equations are meant to illustrate the relations between the interfacial parameters and other concrete parameters. For full verification, more experimental data need to be generated in the future. In the current study, only a single aggregate grading has been employed. In future investigations, the effect of aggregate size distribution should also be considered. Moreover, in this study, the 'aggregate' is arbitrarily defined as particles with projected dimension of 4.75mm or above on the concrete surface. As only part of an aggregate is exposed at the surface, the actual particle size can be much large than 4.75mm, which explains the small values of aggregate content given in Table 1. Such a definition for the 'aggregate' should be re-evaluated in future work.

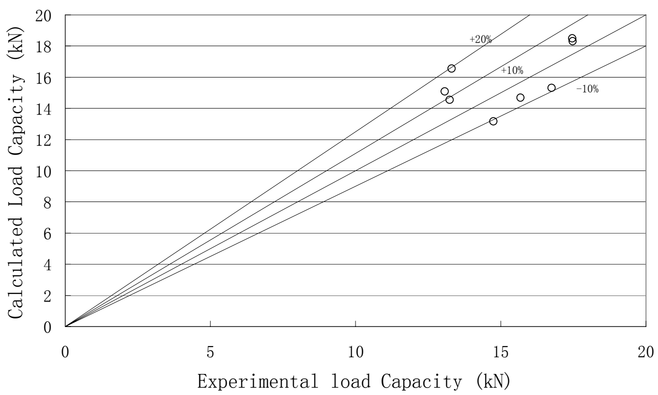

Fig.9 Comparison of calculated bond capacity with experimental results

4 CONCLUSIONS

In this paper, experimental investigations have been conducted to study the effect of the concrete composition on FRP debonding behavior. Our results show little correlation between the interfacial parameters and the compressive strength of concrete. However, the interfacial shear strength (τ_s) correlates well with the surface tensile strength and the residual shear strength has good correlation with the surface tensile strength or the splitting tensile strength. The maximum sliding is mostly governed by the surface tensile strength and the aggregate content. Empirical models are hence proposed to relate τ_s and τ_0 to the surface tensile strength and the maximum sliding 'δ' to the aggregate content and the surface tensile strength. While the current study is far from complete, the results indicate that the composition of concrete (specifically, the aggregate content) is an important factor that should be considered explicitly in the investigation of FRP debonding from a concrete substrate.

REFERENCE

Bizindavyi L. and Neale K.W., (1999) "Transfer length and Bond strengths for composites bonded to concrete." *Journal of composites for construction*, Vol. 3, No. 4. pp.153-160.

Chajes, M.J., Finch, W.W. Januszka T.F. and Thomosh, T.A., (1996) "Bond and force transfer of composite material plates bonded to concrete" *ACI Structural Journal*, vol. 93, No. 2, pp. 231-244.

Chen, J.F., and Teng, J.G. (2001) "Anchorage strength models for FRP and steel plates bonded to concrete." *J. Struct.Engrg.*, Vol.127, No.7, pp.784-791.

Holzenkampfer, O. (1994) "Ingenieurmoddelle des Verbundes geklebter Bewehrung fur Betonbauteile, *Dissertation*, TU Braunschweig.

De Lorenzis, L., Miller, B. and Nanni, A. (2001) "Bond of Fiber-reinforced Polymer Laminates to Concrete" *ACI material Journal*, V. 98, No.3, pp. 256-264.

Leung, C.K.Y., Tung, W.K., (2006) "Three-Parameter Model for Debonding of FRP Plate from Concrete Substrate", *ASCE Journal of Engineering Mechanics*, Vol.132, No.5, pp. 509-518 (2006)

Neubauer U. and Rostasy F. S. (1997) "Design aspects of concrete structures strengthened with externally bonded CFRP plates" *Proceeding of the Seventh International conference on structural Faults and Repairs*, Edited by M.C. Forde, Engineering Technics Press, Edinburgh, UK, pp.109-118.

Taljsten, B. (1997) "Strengthening of beams by plate bonding." *J. Mat. in Civ. Engrg.*, ASCE, 9(4), 206-212.

Van Gemert, D. (1980) "Force transfer in epoxy-bonded steel-concrete joints" *International Journal of Adhesion and Adhesive*, No.1, pp. 67-72.

Yuan, H. Wu, Z.S. and Yoshizawa, H. (2001) "Theoretical solutions on interfacial stress transfer of externally bonded steel/composite laminates." *Journal of Structural Mechanics and Earthquake Engineering*, JSCE, No. 675/1-55, pp.27-39.